HHS Public Access

Author manuscript

Anal Chem. Author manuscript; available in PMC 2017 December 06.

Published in final edited form as:

Anal Chem. 2016 December 06; 88(23): 11691–11698. doi:10.1021/acs.analchem.6b03270.

Capillary Electrophoresis with Laser-Induced Fluorescent Detection of Immunolabeled Individual Autophagy Organelles Isolated from Liver Tissue

Katherine A. Muratore[†], **Heather M. Grundhofer**[‡], and **Edgar A. Arriaga**[‡,*]

[†]Department of Biochemistry, Molecular Biology, and Biophysics, University of Minnesota, Minneapolis, Minnesota 55455, United States

[‡]Department of Chemistry, University of Minnesota, Minneapolis, Minnesota 55455, United States

Abstract

Macroautophagy is a cellular degradation process responsible for the clearance of excess intracellular cargo. Existing methods for bulk quantification of autophagy rely on organelle markers that bind to multiple autophagy organelle types, making it difficult to tease apart the subcellular mechanisms implicated in autophagy dysfunction in liver and other pathologies. To address this issue, methods based on individual organelle measurements are needed. Capillary electrophoresis with laser-induced fluorescent detection (CE-LIF) was previously used to count and determine properties of individual autophagy organelles isolated from an LC3-GFP expressing cell line, but has never been used on autophagy organelles originating from a tissue sample. Here, we used DyLight488-labeled anti-LC3 antibodies to label endogenous LC3 present on organelles isolated from murine liver tissue prior to CE-LIF analysis. We evaluated the ability of this method to detect changes in a known model system of altered autophagy, as well as confirmed the specificity and reproducibility of the antibody in the labeling of autophagy organelles from liver tissue. This is both the first demonstration of CE-LIF to analyze individual organelles labeled with fluorophore-conjugated antibodies, and the first application of individual organelle CE-LIF to measure the properties of autophagy organelles isolated from tissue. The observations described here demonstrate that CE-LIF of immunolabeled autophagy organelles is a powerful technique useful to investigate the complexity of autophagy in any tissue sample of interest.

Graphical Abstract

[*]**Corresponding Author**. arriaga@umn.edu. Phone: +1 612-624-8024.

ASSOCIATED CONTENT

Supporting Information

The Supporting Information is available free of charge on the ACS Publications website at DOI: 10.1021/acs.analchem.6b03270.

Supplementary methods, false positive rate, validation of wild type ATG5$^{(+/+)}$ and knocked-out ATG5$^{(-/-)}$ MEFs, statistical overlap theory of autophagy organelles, QQ plot analysis of autophagy organelles, and linear regression analysis of QQ data (PDF)

The authors declare no competing financial interest.

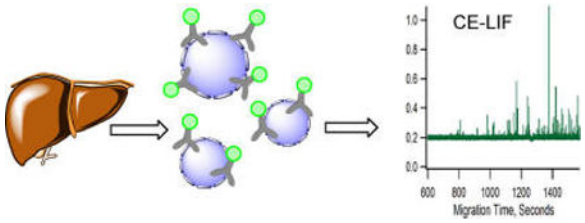

Macroautophagy (referred hereafter as autophagy) is cellular degradation pathway that is critical in the maintenance of cellular homeostasis.[1–3] Loss of autophagy function is implicated in aging[4,5] and numerous liver pathologies, including liver cancer, nonalcoholic and alcoholic fatty liver disease, and viral hepatitis.[6,7] Because these conditions decrease health span, there is a pressing need for reliable and quantitative measurements of autophagy in tissue samples. While there are existing methods for quantifying bulk markers present on autophagy organelles, a method based on individual organelle measurements would reduce bias, by reporting across distributions of properties of organelles in the multiple organelle types present in a given tissue sample.

Current methods for monitoring autophagy are Western blot, transmission electron microscopy (TEM), fluorescent microscopy, and flow cytometry.[8] The most common is a Western blot to monitor the formation of LC3-II, but this method is notorious for incorrect identification of autophagy induction.[8–10]Also, it is impossible to determine from a Western blot whether an increase in LC3-II is indicative of more organelles containing that marker, or an increase in marker density on the surface of existing organelles. TEM enables visualization of autophagy organelle structures,[11–13] but it requires an expert eye for their correct identification.[14] Individual autophagy organelles can be visualized with fluorescent microscopy,[15,16] but counting of individual LC3-II positive organelles is not high-throughput and requires colocalization experiments to determine which autophagy organelles are present. Flow cytometry is a well-defined method for characterizing heterogeneity among individual cells or particles, but its use in detecting individual organelles has been somewhat limited because of high limits of detection. Individual cell[17–19] flow cytometry autophagy assays have been reported, but these methods are contingent on the overexpression of fluorophore-LC3 fusion proteins, which can form aggregates independent of autophagy organelle formation[20] and cannot describe how the reporter distributes among the various autophagy organelle types. Fluorescently labeled primary antibodies have been used to detect individual mitochondria by flow cytometry[21] and capillary cytometry,[22] which is a form of flow cytometry, but these methods have not yet been applied to autophagy organelles and report only individual organelle fluorescence intensities. Other reports have applied flow cytometry to measure individual autophagy organelles also labeled with fluorophore-LC3 conjugates,[18] acidotropic chemical probes,[23] and fluorescently labeled secondary antibodies.[24] In addition to the drawback associated with GFP-fluorophore fusion proteins, acidotropic probes only label acidic autophagy organelles that have fused with lysosomes. Due to the high limit of detection associated with flow cytometry, detection of immunolabeled autophagy organelles has been limited to those labeled with secondary antibodies.[24] Methods based on immunolabeling with primary antibodies for labeling of individual autophagy organelle analysis have not been reported so far.

Capillary electrophoresis with laser-induced fluorescent detection (CE-LIF) has been used to monitor bulk conversion of GFP-LC3-I to GFP-LC3-II in cell extracts[25] as well as individual GFP-LC3-II positive autophagy organelles isolated from C2C12 mouse myoblasts.[26] In addition to autophagy organelles, CE-LIF has been used extensively to determine the numbers and properties of individual mitochondria,[27] liposomes,[28] nuclei[29] and acidic organelles.[30] Advantages of CE-LIF include low limits of detection, which enables the detection of individual fluorescently labeled organelles and the ability to measure individual organelle electrophoretic mobility which enables the investigation of surface heterogeneity among a population of organelles.[26–30]

This Article introduces a new method for monitoring autophagy in tissues using primary antibody labeling and CE-LIF. This technique has been used to analyze immunolabeled peptide hormones,[31] proteins,[32–34] and bacteria,[35] but there has been no report thus far of the application of CE-LIF to analyze immunolabeled organelles. Fluorophore-conjugated primary antibodies have not been used to label individual organelles for CE-LIF analysis, and this technique is capable of measuring the electrophoretic mobility of individual autophagy organelles. In this Article, we describe a method based on labeling of LC3-II with a primary antibody. We first used an established biological model of disrupted autophagy to investigate the sensitivity of the method to changes in autophagy function. Then, we applied the method to quantify properties of individual autophagy organelles isolated from murine liver tissues. Future applications of CE-LIF combined with primary antibody labeling could be used to examine autophagy organelles from tissues obtained from animal models of liver disorders and aging, as well as human tissue biopsies.

EXPERIMENTAL SECTION

Materials, Reagents, Buffers, and Solutions

Sucrose, fluorescein, 4-(2-hydroxyethyl)-1-piperazineethanesulfonic acid (HEPES), mannitol, ethaminetetraacetic acid (EDTA), poly-(vinyl alcohol) (99%+ hydrated, molecular weight 89,000–980,000), dimethyl sulfoxide (DMSO), and ethylene-bis-(oxyethylenenitrilo)tetraacetic acid (EGTA) were obtained from Sigma-Aldrich (St. Louis, MO). Tris base, 4-morpholine-propanesulfonic acid (MOPs), sodium chloride, 10 000 units penicillin, 10 mg streptomycin/mL, Dulbecco's modified Eagle medium (DMEM) high glucose solution, fetal bovine serum, 0.5% trypsin-EDTA (10× solution), AlignFlow flow cytometry beads (2.5 μm), and 200 mM L-glutamine solution (1000×) were obtained from Thermo Fisher Scientific (Waltham, MA). Phosphate buffered saline (PBS, 10× concentration, 1.37 M NaCl, 27 mM KCl, 80 mM Na_2HPO_4, and 20 mM KH_2PO_4, pH 7.4) was obtained from Bio-Rad (Hercules, CA). A polyclonal Dylight488 conjugated rabbit anti-LC3 antibody, was obtained from Novus Biologicals (Littleton, CO). Dylight-488 conjugated rabbit isotype control was obtained from Abcam (Cambridge, UK). Water was purified with a Millipore Synergy UV system (18.2mΩ/cm, Bedford, MA). Cell homogenization buffer consisted of 70 mM sucrose, 215 mM mannitol, 4.31 mM HEPES, and 4.94 mM EDTA, pH 7.4. CE buffer consisted of 250 mM Sucrose, 10 mM HEPES, pH 7.4. PBS was diluted 1:10 in purified water.

Autophagy Organelle Isolation from Cultured Cells and Subsequent Antibody Labeling

ATG5$^{(-/-)}$ and ATG5$^{(+/+)}$ mouse embryonic fibroblasts (MEFs) were a generous gift of Dr. Noboru Mizushima (The University of Toyko, Japan). MEFs were maintained at 37 °C, 5% CO_2 in high glucose DMEM supplemented with 10% fetal bovine serum, 200 μM glutamine, 1000 units penicillin, and 10 μg/mL streptomycin. For propagation, cells were lifted with 0.5% Trypsin-EDTA in PBS and split 1:20 (v/v) into new flasks every 48 h. For autophagy organelle isolation, MEFs were expanded into two 75 cm flasks 48 h prior to experiment day. Cells were harvested, resuspended in 1 mL cell homogenization buffer and disrupted in an ice cold nitrogen cavitation chamber (Parr Instrument Co., Moline, IL). Cells were kept in the chamber at 600 psi for 15 min prior to depressurization and release. All subsequent steps were performed on ice or at 4 °C. The cell lysate was collected in a 50 mL conical tube and centrifuged at 600g for 10 min to pellet unbroken cells and nuclei. The supernatant (postnuclear fraction) was removed to a clean microcentrifuge tube and spun at 10 000*g* for 10 min to pellet autophagy organelles. The organelles were resuspended in 100 μL of CE buffer and incubated with 300 nM DyLight488 anti-LC3 antibody for 1 h on a microcentrifuge tube rotator in a 4 °C cold room. The labeled autophagy organelles were centrifuged at 10 000*g* for 10 min to remove unbound antibody and were resuspended in 200 μL of CE buffer prior to CE-LIF analysis. Protein content of the organelle suspensions was measured by the Pierce BCA Protein Assay Kit (Thermo Fisher Scientific) in accordance with the manufacturer's instructions.

Autophagy Organelle Isolation from Liver and Subsequent Antibody Labeling

All mice were housed in a designated clean facility and treated in accordance with protocols approved by the Institutional Animal Care and Use Committee at the University of Minnesota. Autophagy organelles were prepared from the livers of male and female adult mice, using a procedure adapted from a published mitochondrial isolation method.[36] Each CE-LIF experiment was performed on autophagy organelles isolated from a single mouse liver. The mouse was euthanized and the liver was removed and placed into 10 mL liver homogenization buffer (10 mM Tris, 1 mM EGTA, 10 mM MOPS, 200 mM Sucrose) on ice. The liver remained on ice or at 4 °C unless otherwise noted. The liver was moved to a small Petri dish and sliced into 1 mm pieces using a flat razor blade. The liver pieces were rinsed with liver homogenization buffer until free of blood and resuspended in fresh liver homogenization buffer at 1:5 (w/v) and transferred to a 15 mL glass homogenization tube (Wheaton, Millville, NJ). The liver suspension was homogenized in a tight fitting motor driven Teflon pestle (Wheaton) operated at 2200 rpm for four strokes. The homogenate was centrifuged at 600g for 10 min and the cloudy supernatant (postnuclear fraction), containing autophagy organelles, was transferred to clean 1 mL microcentrifuge tubes. The post nuclear fractions were centrifuged at 10,000g for 10 min to pellet autophagy organelles. Each pellet was resuspended in in 500 μL CE buffer and combined into a 15 mL conical tube. This step served to concentrate the sample prior to organelle labeling.

For antibody labeling, the organelle suspension was separated in to 100 μl aliquots and incubated with DyLight488 labeled anti-LC3 antibody or DyLight488 isotype control at concentrations ranging from 5 to 300 nM for 1 h on a microcentrifuge tube rotator in the 4 °C cold room. The labeled autophagy organelles were centrifuged at 10,000g for 10 min to

remove unbound antibody and were resuspended in 100 μL CE buffer, and diluted 1:50 (v/v) in CE-buffer prior to CE-LIF analysis or diluted 1:2500 (v/v) in CE buffer prior to capillary cytometry analysis.

Instrumentation and Alignment

A previously described, home-built instrument[28] with post capillary sheath flow LIF detection was used to determine numbers of autophagy organelles, DyLight488 intensity of each organelle, and electrophoretic mobility of each organelle. To align the optics for consistent fluorescent response, the optics were adjusted until the fluorescence intensities of individual alignment beads (AlignFlow, Molecular Probes, Thermo Fisher Scientific) maintained a relative standard deviation within the manufacturers specifications (~30%).[22,26] Excitation of all samples resulted from a 488 nm 12 mW argon-ion laser (JDS Uniphase, San Jose, CA). Dylight488 emission was selected by a 525 ± 25 nm band-pass filter (Omega Optical, Brattleboro, VT). Emitted photons were detected by photomultiplier tube (R1477, Hamamatsu, Bridgewater, NJ) and the output was digitized at 200 Hz with a NiDaq I/O board (PCI-MIO-16XE-50, National Instruments, Austin, TX), collected with customized LabVIEW 5.1 software (National Instruments) and stored as binary files.

For CE-LIF analysis, a sample volume containing organelles was introduced into a 30 μm inner-diameter fused silica glass capillary (Polymicro, Phoenix AZ) via siphoning (104 cm height, 10 s injection). Capillaries were coated in-house with poly vinyl alcohol to decrease electro osmotic flow and prevent absorption of organelles into capillary walls.[37] Capillary electrophoresis separations were performed at −300 V/cm for 30 min for liver samples and 40 min for MEF samples.

For capillary cytometry analysis, organelles were passed through 30 μM inner-diameter uncoated fused silica glass capillary (Polymicro) at a rate of 20 nL/min maintained by the application of external pressure (10 ± 1 kPa) provided by a nitrogen pressurized Erlenmeyer flask, as described previously.[22] Unlike CE-LIF, capillary cytometry does not provide the electrophoretic mobility of individual organelles. Constant introduction of organelles into the capillary by application of external pressure allows a larger amount of organelles to be analyzed in a shorter time than CE-LIF analysis. Thus, capillary cytometry was used to evaluate multiple antibody concentrations on a single day, as our measures of antibody labeling were only dependent on event intensity. Capillary cytometry analyses were performed for 20 min.

To eliminate carryover between samples in both CE-LIF and capillary cytometry experiments, methanol was passed through the capillary for 5 min to remove biological material and CE buffer was passed through the capillary for 5 min to reequilibrate the capillary. At the end of each experiment, methanol was passed the capillary for 5 min to remove biological material and air was passed through the capillary to dry it prior to storage.

Data Analysis

Peak time, peak width, and peak intensity of all organelle events was obtained as previously described from the binary files using IgorPro software (WaveMetrics, Oswego, Oregon), with in-house written algorithms.[30] The program selected peaks with signal intensities

higher than a given threshold. As previously reported,[30,38] the electropherogram (CE-LIF) or flowgram (capillary cytometry) was divided into “premigration” and “collection” windows. Only false positives are detected in the premigration window, while both false and true positives are detected in the collection window. The initial threshold was set to 3 times the standard deviation (σ) of the background in the premigration window and then adjusted up to either 4σ or 5σ so that the number of events detected was ~5–10% of those observed with a 3σ threshold. After selection of a final threshold, the total number of organelle events observed in the collection window was corrected for number of events (false positives) observed in the premigration window using the equation

$$O_c = O_T - \left(\frac{N}{P}\right) W \quad (1)$$

where O_T is the total number of organelles observed in the collection window, N is the number of false positive events in the premigration window, P is the length of the premigration window in seconds, and W is the length of the collection window in seconds (Figure S1).

To account for variations in the amount of protein in organelles prepared from ATG5$^{(-/-)}$ MEFs and ATG5$^{(+/+)}$ MEFs, peak numbers were normalized to the nanograms of protein injected, as described previously.[26] The calculated electrophoretic mobilities of individual organelles are affected by run-to-run fluctuations. Thus, a fluorescein standard was injected with each organelle separation, and the previously reported ($-3.0 \pm 0.1 \times 10^{-4}$ cm^2 V^{-1} s^{-1})[39] and observed mobilities of fluorescein were used to correct the mobilities of observed organelle events, as described before.[26] To eliminate day-to-day variations in detector sensitivity, each experiment was performed on a single day.

The coupling of fluorophores to antibodies is variable and the fluorophore/protein (F/P) molar ratios can differ between antibody lots. To account for variations in between DyLight488 labeled anti-LC3 and DyLight488 labeled isotype control antibodies compared in a single experiment, intensity values were normalized to the F/P ratio. The corresponding F/P ratio for each antibody used was calculated as

$$\frac{F}{P} = \frac{A_{\text{maxDyLight488}}}{\varepsilon'_{\text{DyLight488}} \times [\text{IgG}]} \quad (2)$$

where $A_{\text{maxDylight488}}$ is the absorbance of the dye measured at its wavelength maximum (493 nm), $\varepsilon'_{\text{Dylight488}}$ is the extinction coefficient of the dye (70 000 M^{-1} cm^{-1}), and [IgG] is the concentration of the antibody, measured from absorbance at 280 nm, corrected for the contribution of DyLight488. The normalized intensity values, I_N, were corrected to the F/P ratio using the equation

$$I_N = \begin{cases} I \times \frac{F_2/P_2}{F_1/P_1}, & \frac{F_2}{P_2} < \frac{F_1}{P_1} \\ I \times \frac{F_1/P_1}{F_2/P_2}, & \frac{F_1}{P_1} > \frac{F_2}{P_2} \end{cases} \quad (3)$$

where I represents the DyLight488 intensity measured in arbitrary units (A.U.) and the two antibodies used in the experiment have F/P ratios F_1/P_1 and F_2/P_2.

Histograms and quantile–quantile (QQ) plots were used to compare distributions of organelle electrophoretic mobilities and DyLight488 intensities. QQ plots are created by plotting the fifth through 95th percentiles from two sample distributions. If the two distributions are similar, their QQ plot approaches an $X = Y$ line. Three technical replicate separations of autophagy organelles labeled with DyLight 488 anti-LC3 and Dylight488 isotype control were performed in alternating order on a single day over a period of 6 h. For visual evaluation of distribution reproducibility among technical replicates, the QQ plot was produced by graphing the fifth through 95th percentiles of each individual replicate distribution versus the 5th through 95th percentile of the pooled distribution. Linear regression also was used for quantitative evaluation of distribution reproducibility among technical replicates. Confidence intervals were constructed for hypothesis testing.

Statistical overlap theory (SOT) was applied to predict the overlap of individual events[40] and determine whether the number of observed peaks was an adequate representation of the number of organelles present in the sample. This technique was previously used to predict overlap of individual mitochondria[22,41,42] and autophagy-related organelles.[26] Briefly, the peaks in each electropherogram or flowgram were partitioned into bins. A maximum number of peaks allowed per bin, $m_{critical}$, was calculated based on the bin length (X) and the standard deviation of peak widths in the bin (σ).[42] If the number of observed peaks, p, exceeds $m_{critical}$, then overlap precluded an accurate count of events. If p is less than $m_{critical}$, then the peaks in the bin have a 90% probability of falling within a 95% confidence interval of representing a single event. In bins where p exceeded $m_{critical}$, we used $m_{critical}$ as a conservative measure of the number of organelle events present in that bin. As there is no relationship between event time and event intensity, events from bins in large overlap were eliminated prior to comparison of intensity distributions. As electrophoretic mobility is calculated from event time, we were unable to remove events from bins in large overlap prior to comparison of electrophoretic mobility distributions.

Safety Information

Biosafety level 1 procedures were followed when working with MEFs and murine liver tissue. Appropriate PPE included a lab coat, safety glasses, and gloves. All biological waste was treated with 10% bleach prior to disposal in the laboratory sink with copious amounts of water.

RESULTS AND DISCUSSION

Analysis of Individual Organelles Labeled with Anti-LC3 Antibodies

Most methods to monitor autophagy rely on the use of anti-LC3 antibodies for the measurement of LC3-II, which is the lipidated form of microtubule-associated protein 1*A*/1B-light chain 3 (LC3), which is required for the formation of mammalian autophagosomes.[43] Similarly, a method for immunolabeling endogenous LC3 present on individual autophagy organelles would enable CE-LIF of individual autophagy organelles possible in any tissue or cell line that is amenable to organelle isolation, making it possible to compare the properties of LC3 positive individual organelles.

The first focus of this report was to determine the suitability of antibodies as organelle labels for CE-LIF analysis, and to detect changes in distributions of individual organelle electrophoretic mobility and DyLight488 anti-LC3 levels in a model system of altered autophagy. Prior work demonstrated the use of CE-LIF to measure the numbers of GFP-LC3 containing autophagy organelles and determine their properties.[26] The major limitation of such method was its reliance on overexpression of LC3-GFP fusion proteins, which make the technique not applicable to tissues. Labeling of organelle preparation from mouse liver with DyLight488 anti-LC3, followed by CE-LIF analysis, showed that individual organelles appeared in electropherograms as individual peaks (Figure 1A) with their width determined by the time the organelle took to pass through the laser beam in the LIF detector. The average peak width (15 ± 3 ms; avg ± std deviation, n = 819 peaks) is compatible with the travel time through the laser beam and in agreement with our previous report on the analysis of GFP-LC3 labeled autophagy organelles (peak width 36 ± 16 ms; avg ± std deviation, n = 12,567 peaks).[25] That individual autophagy organelles appear as narrow peaks (Figure 1C) when labeled with DyLight488 anti-LC3, is consistent with the fact that such label is bound to a particle and not free in solution. Because the DyLight488 anti-LC3 antibody also binds to LC3-I free in the cytosol, the antibody-LC3 complex could have been detected as a wide peak, similar to what we observe for fluorescein, which was coinjected with the organelle sample as a standard (Figure 1D). It is worth mentioning that a band for DyLight488 labeled LC3-I was not detected, because cytosolic proteins are removed in the organelle isolation procedure. Thus, the signal intensity of each peak event refers to the amount of DyLight488 present on an individual organelle.

On the other hand, not all organelles detected correspond to autophagy organelles. Antibodies may display nonspecific binding to different epitopes other than the one it was raised against.[44] To correct for nonspecific binding, isotype controls do not recognize the epitope of interest have been used in flow cytometry.[45] In this study, we selected a DyLight488-labeled isotype as control for nonspecific binding. When the organelle sample was treated with DyLight488 isotype antibody that does not bind to LC3, a few events were detected (30 events), suggesting that some organelles are labeled due to nonspecific binding (Figure 1B). This is a small fraction relative to labeling with anti-LC3 antibodies (~14%) that can be easily corrected through data processing as described below.

A unique aspect of the analysis of individual autophagy organelles by CE-LIF is the determination of their electrophoretic mobilities. As described below each organelle has a

unique electrophoretic mobility, which is heavily influenced by its surface composition,[28] and results in a different migration time (Figure 1A). Thus, the results shown indicate that antibody labeling of autophagy organelles enables measurement not only of the number of organelles, and their individual fluorescence intensities resulting from immunolabeling, but also their electrophoretic mobilities.

To determine if this new method could detect differences in the properties of autophagy organelles in a well-characterized biological system, we analyzed cells deficient in autophagy ($ATG5^{(-/-)}$ MEFs) and an appropriate control ($ATG5^{(+/+)}$ MEFs). LC3 is recruited to the autophagosome membrane in an ATG5 dependent manner,[46,47] and cells deficient in ATG5 will have a decrease in autophagosome formation. To validate this cell system, Western blot analysis indicated that $ATG5^{(-/-)}$ cells ATG5 protein levels were below the limit of detection of the method (~15 fg, Figure S2). Quantitative reverse-transcriptase polymerase-chain reaction (q-RT-PCR) indicated that $ATG5^{(-/-)}$ cells had a 99.960 ± 0.001% (mean ± SEM) reduction in ATG5 gene expression (Figure S2). CE-LIF analysis of organelles isolated from $ATG5^{(-/-)}$ MEFs and $ATG5^{(+/+)}$ MEFs and labeled with DyLight488 anti-LC3 provided (1) the number of organelles in the sample, (2) the distribution of organelle intensities, and (3) the distributions of organelle electrophoretic mobilities.

Application of the statistical overlap theory (SOT) to the separations of organelles isolated from $ATG5^{(+/+)}$ or $ATG5^{(-/-)}$ MEFs (Figure S3), indicated that it was feasible to estimate organelle counts in each sample. As expected, samples from $ATG5^{(+/+)}$ cells had a higher number of total autophagy organelles than $ATG5^{(-/-)}$ cells (745 and 22 events, respectively) when normalized to sample protein content. Correction for false positive rate (eq 1), resulted in 729 organelles for $ATG5^{(+/+)}$ and 0 for $ATG5^{(-/-)}$ cells.

This is in agreement with previously reported phenotype of ATG5 (−/−) mouse embryonic stem cells that have impaired autophagosome formation, and an estimated ~45 fold decrease in LC3-II formation.[48]

Histograms were used to visualize distributions of individual organelle intensities (Figure 2A) and individual organelle electrophoretic mobilities (Figure 2B) from $ATG5^{(+/+)}$ MEFs. As the corrected number of autophagy organelles in $ATG5^{(-/-)}$ MEFs was 0, the distribution of events observed in that sample (false positives), were subtracted from the $ATG5^{(+/+)}$ the MEFs distributions. The range in the intensity distribution (Figure 2A) illustrates the heterogeneity in LC3-II contents in autophagy organelles. Similarly, the distribution of electrophoretic mobilities is representative of the surface composition of autophagy organelles, primarily determined by the proteins and lipids that are present in their surface.[26] Thus, the CE-LIF results of the analysis of organelles isolated from $ATG^{(+/+)}$ MEFs and $ATG5^{(-/-)}$ MEFs provide clear differences in heterogeneity of a biologically relevant model system of altered autophagy.

Immunolabeling Specificity toward Individual Organelles Isolated from Murine Liver Tissue

Next, we investigated the effect of nonspecific labeling on the CE-LIF analysis of autophagy organelles isolated from murine liver tissue. Organelles were labeled with 300 nM

DyLight488-conjugated anti-LC3 antibody or DyLight488-conjugated isotype control prior to CE-LIF analysis. This relatively high concentration of antibodies ensured detection of a sufficiently high number of events for each of the antibodies. After normalizing for amount of protein contents in each sample, correcting for false positives (eq 1), adjusting peak intensities for F/P ratios (eqs 2 and 3), and confirming that peak overlap was not an issue (Figure S4), the numbers of detected events were 773 and 726 in the samples treated with DyLight488-conjugated anti-LC3 antibody and the DyLight 488-conjugated isotype control, respectively. These high numbers of events detected, made possible comparisons of individual organelle intensity and electrophoretic mobility distributions.

The distributions of event intensities were compared using a QQ plot (Figure 3A). The quantiles were represented as markers at 5th, 10th, 15th, …, percentiles. As expected, the general trend was positive deviation from the diagonal, indicating that nonspecific binding events are overall less intense than organelles labeled with the specific antibody. Furthermore, the clear deviation from the diagonal for events falling in the 65th–100th percentiles suggest that such events represent specific binding of the DyLight488 anti-LC3 antibody.

Because the specific binding of the DyLight488 anti-LC3 and the nonspecific binding of the DyLight488 isotype represent different organelle populations, we also anticipated different electrophoretic mobility distributions of the detected individual events. The organelles detected due to the specific binding of the DyLight488 anti-LC3 are associated with the autophagy process and include other organelles such as phagophores and autolysosomes that have LC3-II in their membranes.[10,49,50] In contrast, DyLight488 isotype labeling does not represent any particular organelle type. Indeed, the QQ of electrophoretic mobility distributions suggested that the electrophoretic mobility (i.e., surface charge density) of the autophagy organelles is predominantly more negative than that nonspecific binding events over the 10th– 90th percentile range ((Figure 3B). Because antibodies are likely protonated (positive charge) during the separation, (isoelectric points of antibodies are typically between 8 and 11[51] and the pH of the separation buffer was 7.4), binding of DyLight488 anti-LC3 antibodies to autophagy organelles cannot explain the unique negative surface charge density we observed for such organelles.

In summary, comparisons of individual event intensities and electrophoretic mobilities distributions confirm that Dy-Light488 anti-LC3 antibody and the DyLight488 isotype represent different organelle populations. However, the high number of nonspecific binding events required optimization of the antibody concentrations used in labeling.

Titration of Antibody Concentration to Maximize Differences between Anti-LC3 and Isotype-Labeled Organelles

The polyclonal anti-LC3 antibody used here (undefined K_D), which is the most commonly used antibody for LC3 detection, required empirical optimization. Capillary cytometry was used to investigate differences in numbers and intensity of individual organelles labeled with four different DyLight488-conjugated anti-LC3 antibody and Dylight488-conjugated isotype control concentrations. Although capillary cytometry does not provide electrophoretic mobility values, it reduces the analysis time per sample from 30 to 40 to 20 min, which

made possible analysis of organelles labeled with 5 nM, 50 nM, 150 nM, and 300 nM DyLight488-conjugated anti-LC3 antibody or DyLight488-conjugated isotype control on 1 day.

The corrected number of organelle events (c.f., eqs 1–3) tended to increase with anti-LC3 concentration, but remained relatively low among the various isotype concentrations tested (Figure 4A). Except for 5 nM, the number of observed organelle events were higher for labeling with the anti-LC3 antibody than that of labeling with the isotype control suggesting that any of these concentrations could be adequate for subsequent experiments. Upon closer examination, it became apparent that numbers of observed events at 150 nM and 300 nM anti-LC3 concentrations displayed peak overlap (Figure S5). Furthermore, the number of nonspecific binding events are relatively significant when labeling with antibodies at the high end of the concentration range (see previous subsection) and there may be unwanted formation of antibody aggregates. Thus, although labeling with a high concentration of anti-LC3 antibody would favor detection of autophagy organelles with low LC3-II copies on their surface, the comparison of the number of organelles favored selection of 50 nM anti-LC3 antibody and isotype concentrations in subsequent studies

Comparison of intensities of organelles labeled with the anti-LC3 and isotype control at the concentrations described above also suggested that 50 nM antibody concentrations were adequate. The differences in median intensities of individual organelles labeled with the anti-LC3 and the isotype control show that the maximum difference is at this concentration (Figure 4B). QQ plots comparing their respective intensity distributions also show the same (Figures 4C and S5). It is important to note that such plots show no difference for 5 nM antibody concentrations (Figure S5E) and that the plots become unreliable when there is significant peak overlap as determined by SOT (Figure S5C, S5D, S5F, and S5G). Thus, it is clear that a 50 nM antibody concentration results in a large positive shift in overall intensity distribution between the anti-LC3 antibody and isotype control (Figure 4C). Thus, comparisons of event numbers and individual peak intensities suggest that 50 nM was the most suitable antibody concentration for evaluating specific binding of the Dy-Light488-conjugated anti LC3 antibody.

Reproducibility of CE-LIF Analysis of Tissue Organelles Using Optimized Antibody Concentrations

To investigate reproducibility of CE-LIF analysis we compared the number of events, individual organelle intensity distributions, and individual organelle electrophoretic mobility distributions resulting from replicate injections of a single preparation of organelles that were labeled with 50 nM DyLight488 anti-LC3 or 50 nM DyLight488 isotype control.

After correction for false positive rate (eq 1), F/P ratios (eqs 2 and 3) and confirming that there was no peak overlap (Figure S6) there were 283 ± 76 and 26 ± 8 organelle events (mean ± std dev; $n = 3$ injections) when labeled with DyLight488-conjugated anti-LC3 antibody and DyLight488-conjugated isotype control, respectively. On the basis of these results, nonspecific binding is ~9% relative to specific binding, when using 50 nM antibody concentration.

Reproducibility of individual organelle intensity and electrophoretic mobility distributions were assessed using QQ plots (Figures 5A and B, respectively). The percentiles of each technical replicate (*y*-axis) were visually similar to the replicates pooled (*x*-axis). If two given distributions of two technical replicates were identical, the slope of a linear fit of their QQ plot should be ~1. To investigate if this was the case, we applied linear regression analysis and made pairwise comparisons of the slopes (Figure S7). The mean slopes were 0.8 ± 0.1 and 1.20 ± 0.08 (mean ± std dev; $n = 3$ comparisons) for the QQ plots of intensity and electrophoretic mobility distributions, respectively. The differences between slopes were statistically significant only for the intensity distributions and not for the electrophoretic mobility distributions (Figure S7). This is representative of the variability expected for CE-LIF analysis of organelles conducted over 6 h in which the labeling is done through chemical probes or genetically engineered proteins. Thus, labeling of 50 nM DyLight488 anti-LC3 was adequate for the CE-LIF analysis of autophagy organelles isolated from liver tissue, thereby establishing a new method for immunolabeling of organelles for individual organelle analysis by CE-LIF.

CONCLUDING REMARKS

While CE-LIF has been successfully applied to immunolabeled peptide hormones,[31] proteins,[32–34] and bacteria,[35] here we introduce the use of immunolabeling for analysis of individual organelles by CE-LIF. To our knowledge, primary antibodies have never been used to label individual organelles for subsequent analysis by CE-LIF or flow cytometry. Because the antibody is specific molecular target (e.g., LC3), this method is capable of reporting on the heterogeneity on the abundance of such target in individual organelles and should be amenable to analysis of other murine tissue samples. The electrophoretic mobility provides a glimpse at the complex mixture of organelles having LC3-II at their surface. Future work using multiple labeling with other antibodies specific for various autophagy-organelle types and detection in multichannel LIF detectors[52] would enable further identification of autophagy organelles with LC3-II at their surface. After proper selection and validation of antibodies, the method could also be easily extended to investigate the distribution of other molecular targets in organelles isolated including those from human tissue biopsies. Future methodological developments could include the characterization of K_D values of other organelle-specific ligands including monoclonal antibodies, recombinant antibodies, and aptamers.

Supplementary Material

Refer to Web version on PubMed Central for supplementary material.

Acknowledgments

We thank Dr. M. Kyba from the Department of Pediatrics and Dr. D. Lowe from the Department of Physiology at the University of Minnesota for providing mice for the autophagy organelle isolation. We thank Dr. N. Mizushima from the University of Tokyo for the generous gift of $ATG5^{(-/-)}$ and $ATG5^{(+/+)}$ MEF cells, provided to us by Dr. D. Kim from the Department of Biochemistry, Molecular Biology, and Biophysics at the University of Minnesota. K.A.M., H.M.G., and E.A.A. thank the National Institutes of Health (Grants RO1-AG020866, T32-GM008700, and T32-AG029796).

REFERENCES

1. Lilienbaum A. Int. J. Biochem. Mol. Biol. 2013; 4(1):1–26. [PubMed: 23638318]
2. Kaur J, Debnath J. Nat. Rev. Mol. Cell Biol. 2015; 16(8):461–472. [PubMed: 26177004]
3. He C, Klionsky DJ. Annu. Rev. Genet. 2009; 43:67–93. [PubMed: 19653858]
4. Cuervo AM, Bergamini E, Brunk UT, Dröge W, French M, Terman A. Autophagy. 2005; 1(3):131–140. [PubMed: 16874025]
5. Rubinsztein DC, Mariño G, Kroemer G. Cell. 2011; 146(5):682–695. [PubMed: 21884931]
6. Cursio R, Colosetti P, Codogno P, Cuervo AM, Shen HM. BioMed Res. Int. 2015; 2015:1–2.
7. Rautou P-E, Mansouri A, Lebrec D, Durand F, Valla D, Moreau R. J. Hepatol. 2010; 53:1123–1134. [PubMed: 20810185]
8. Barth S, Glick D, Macleod KF. J. Pathol. 2010; 221(2):117–124. [PubMed: 20225337]
9. Mizushima N, Yoshimori T. Autophagy. 2007; 3(6):542–545. [PubMed: 17611390]
10. Klionsky DJ, et al. Autophagy. 2012; 8(4):445–544. [PubMed: 22966490]
11. Ashford TP, Porter KR. J. Cell Biol. 1962; 12:198–202. [PubMed: 13862833]
12. Deter RL, De Duve C. J. Cell Biol. 1967; 33(2):437–449. [PubMed: 4292315]
13. Eskelinen EL. Methods Mol. Biol. 2008; 445(11):11–28. [PubMed: 18425441]
14. Eskelinen EL. Autophagy. 2008; 4(2):257–260. [PubMed: 17986849]
15. Kadowaki M, Karim MR. Methods Enzymol. 2009; 452:199–213. [PubMed: 19200884]
16. Kimura S, Noda T, Yoshimori T. Autophagy. 2007; 3(5):452–460. [PubMed: 17534139]
17. Eng KE, Panas MD, Karlsson Hedestam GB, McInerney GM. Autophagy. 2010; 6(5):634–641. [PubMed: 20458170]
18. Shvets E, Fass E, Elazar Z. Autophagy. 2008; 4(5):621–628. [PubMed: 18376137]
19. Hundeshagen P, Hamacher-Brady A, Eils R, Brady NR. BMC Biol. 2011; 9(1):38. [PubMed: 21635740]
20. Kuma A, Matsui M, Mizushima N. Autophagy. 2007; 3(4):323–328. [PubMed: 17387262]
21. Zhang S, Zhu S, Yang L, Zheng Y, Gao M, Wang S, Zeng J, Yan X. Anal. Chem. 2012; 84:6421–6428. [PubMed: 22784011]
22. Taylor TH, Frost NW, Bowser MT, Arriaga EA. Anal. Bioanal. Chem. 2014; 406(6):1683–1691. [PubMed: 24481619]
23. Degtyarev M, Reichelt M, Lin K. PLoS One. 2014; 9(1) No. e87707.
24. Koga H, Kaushik S, Cuervo AM. FASEB J. 2010; 24(8):3052–3065. [PubMed: 20375270]
25. Jin Y, Chen C, Meng L, Chen J, Li M, Zhu Z, Lin J. Analyst. 2012; 137(23):5571–5575. [PubMed: 23057067]
26. Satori CP, Arriaga EA. Anal. Chem. 2013; 85(23):11391–11400. [PubMed: 24164243]
27. Duffy C, Fuller K, Malvey M, O'Kennedy R, Arriaga EA. Anal. Chem. 2002; 74(1):171–176. [PubMed: 11795787]
28. Duffy CF, Gafoor S, Richards DP, Admadzadeh H, O'Kennedy R, Arriaga EA. Anal. Chem. 2001; 73(8):1855–1861. [PubMed: 11338602]
29. Gunasekera N, Olson K, Musier-Forsyth K, Arriaga EA. Anal. Chem. 2004; 76(3):655–662. [PubMed: 14750860]
30. Chen Y, Arriaga EA. Anal. Chem. 2006; 78(3):820–826. [PubMed: 16448056]
31. Shimura K, Waki T, Okada M, Toda T, Kimoto I, Kasai KI. Electrophoresis. 2006; 27(10):1886–1894. [PubMed: 16703627]
32. Zhang H, Jin W. Electrophoresis. 2004; 25(7–8):1090–1095. [PubMed: 15095451]
33. Lacroix M, Poinsot V, Fournier C, Couderc F. Electrophoresis. 2005; 26(13):2608–2621. [PubMed: 15948219]
34. Yang WC, Schmerr MJ, Jackman R, Bodemer W, Yeung ES. Anal. Chem. 2005; 77(14):4489–4494. [PubMed: 16013864]
35. Shintani T, Torimura M, et al. FEMS Microbiol. Lett. 2002; 210:245–249. [PubMed: 12044682]
36. Frezza C, Cipolat S, Scorrano L. Nat. Protoc. 2007; 2(2):287–295. [PubMed: 17406588]

37. Whiting CE, Arriaga EA. Electrophoresis. 2006; 27(22):4523–4531. [PubMed: 17117462]
38. Anderson AB, Xiong G, Arriaga EA. J. Am. Chem. Soc. 2004; 126(30):9168–9169. [PubMed: 15281791]
39. Kostal V, Fonslow BR, Arriaga EA, Bowser MT. Anal. Chem. 2009; 81(22):9267–9273. [PubMed: 19908903]
40. Davis JM, Arriaga EA. J. Chromatogr. A. 2009; 1216(35):6335–6342. [PubMed: 19632681]
41. Davis JM, Arriaga EA. Anal. Chem. 2010; 82(1):307–315. [PubMed: 20041721]
42. Wolken GG, Kostal V, Arriaga EA. Anal. Chem. 2011; 83(2):612–618. [PubMed: 21192658]
43. Kabeya Y, Mizushima N. EMBO J. 2000; 19(21):5720–5728. [PubMed: 11060023]
44. Baker M. Nature. 2015; 521:274–275. [PubMed: 25993940]
45. Maecker HT, Trotter J. Cytometry, Part A. 2006; 69A:1037–1042.
46. Mizushima N, Yoshimori T, Ohsumi Y. Annu. Rev. Cell Dev. Biol. 2011; 27:107–132. [PubMed: 21801009]
47. Mizushima N, Ohsumi Y, Yoshimori T. Cell Struct. Funct. 2002; 27:421–429. [PubMed: 12576635]
48. Mizushima N, Yamamoto A, Hatano M, Kobayashi Y, Kabeya Y, Suzuki K, Tokuhisa T, Ohsumi Y, Yoshimori T. J. Cell Biol. 2001; 152(4):657–668. [PubMed: 11266458]
49. Tanida I, Ueno T, Kominami E. Int. J. Biochem. Cell Biol. 2004; 36(12):2503–2518. [PubMed: 15325588]
50. Mizushima N. Genes Dev. 2007; 21:2861–2873. [PubMed: 18006683]
51. Boswell CA, Tesar DB, Mukhyala K, Theil FP, Fielder PJ, Khawli LA. Bioconjugate Chem. 2010; 21(12):2153–2163.
52. Dada OO, Essaka DC, Hindsgaul O, Palcic MM, Prendergast J, Schnaar RL, Dovichi NJ. Anal. Chem. 2011; 83(7):2748–2753. [PubMed: 21410138]

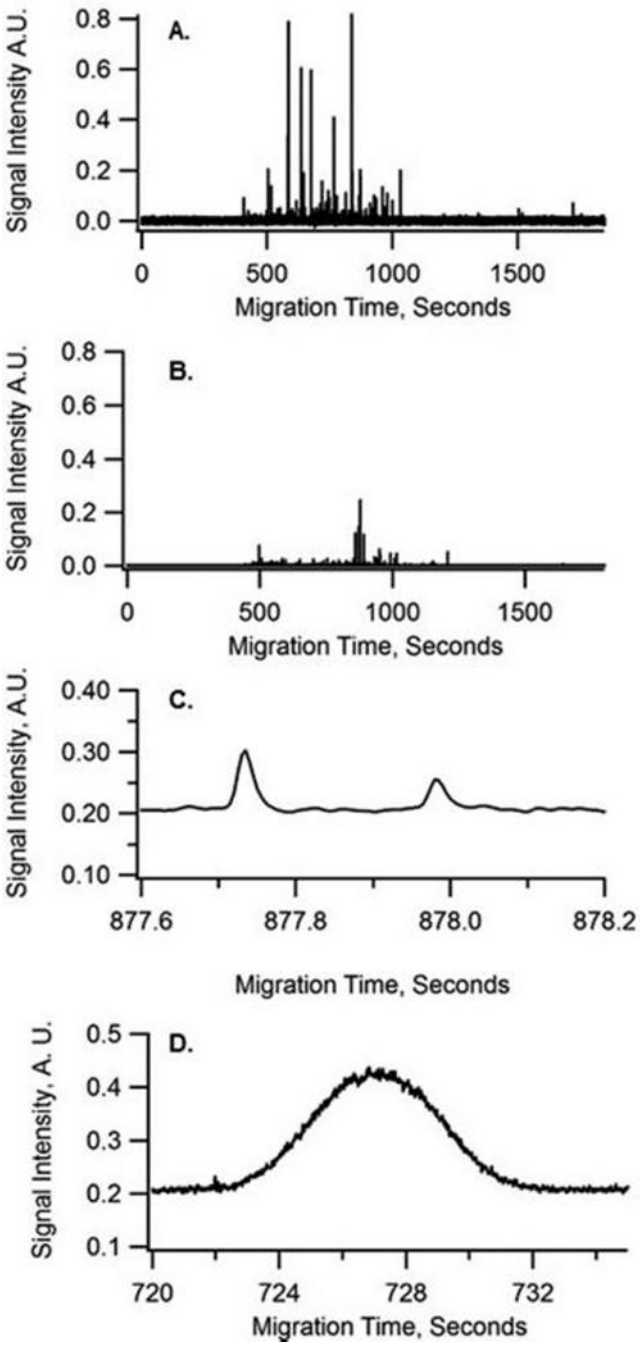

Figure 1.

Representative electropherograms of individual autophagy organelles. (A) Autophagy organelles labeled with 50 nM DyLight-488 anti-LC3, $n = 208$ peaks. (B) Organelle fraction labeled with 50 nM DyLight488 isotype control, $n = 30$ peaks. Samples are from murine mouse liver. Organelles appeared as individual peaks after a premigration window of ~400 s. Threshold was set to 4σ. Buffer was 250 mM Sucrose, 10 mM HEPES pH 7.2. Excitation was from a 12 mW 488 nm argon-ion laser. Fluorescence detection, 525df25 band-pass filter. Hydrodynamic injection, 10 s, 11.11 kPa pressure drop. Capillary ID, 30 μm. (C)

Expansion of Part A showing individual organelle peaks. (D). Fluorescein peak (9.6-s wide), resulting from coinjection of internal standard, processed after removal of individual peaks from electropherogram using a median filter.

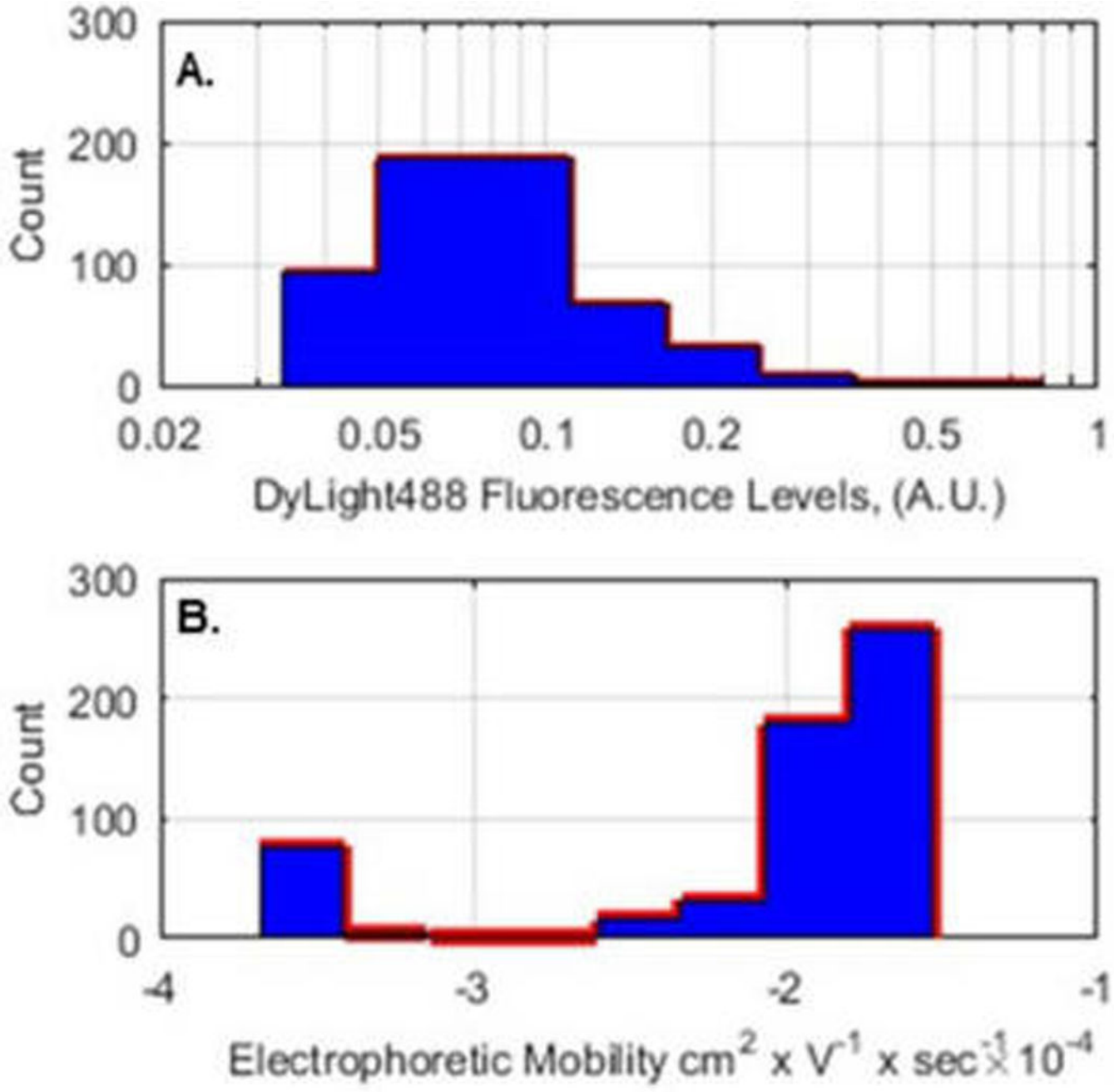

Figure 2.

Autophagy organelle DyLight488 intensity and electrophoretic mobility distributions from ATG5$^{(+/+)}$ MEFs. (A). Intensity distribution from ATG5$^{(+/+)}$ MEFs, n = 745 events. (B) Electrophoretic mobility distribution from ATG5$^{(+/+)}$ MEFs, n = 745 events. Data were acquired using conditions described in Figure 1. Data from ATG$^{(-/-)}$ MEFs were subtracted bin by bin in both distributions.

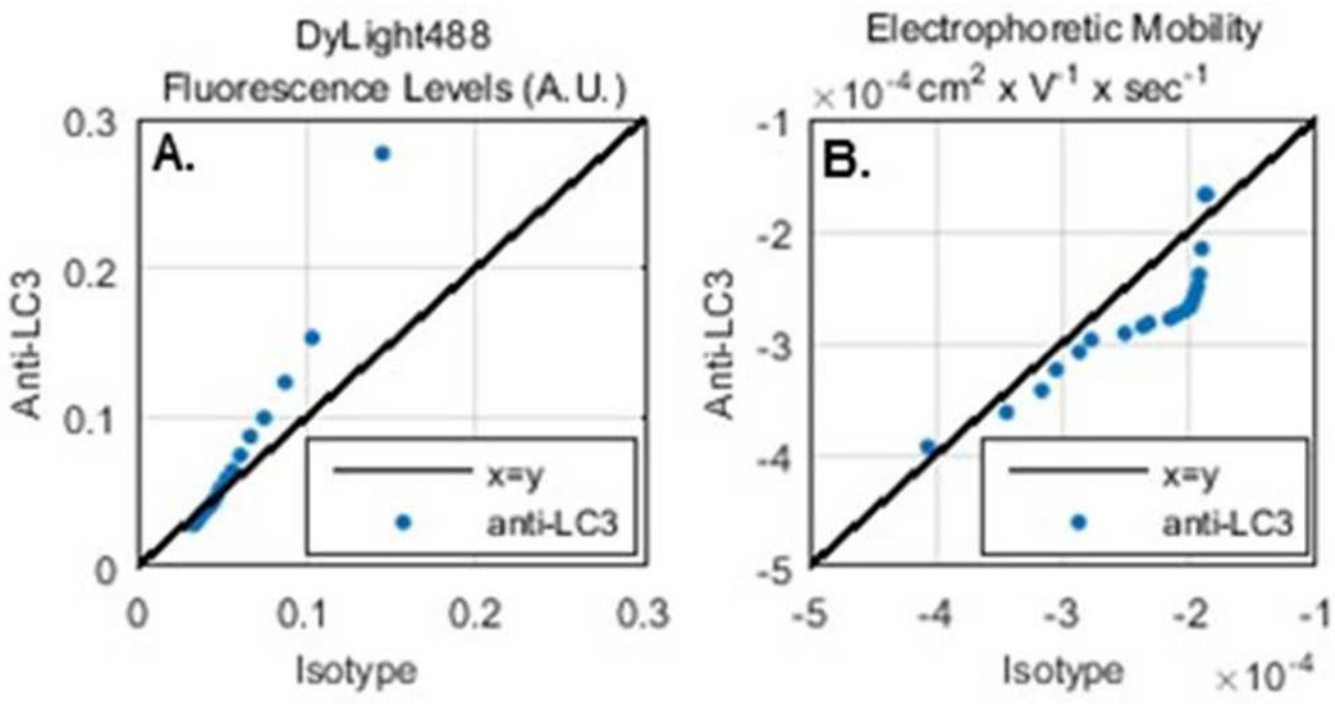

Figure 3.

Comparison of intensity and electrophoretic mobility distributions of organelles labeled with DyLight488 Anti-LC3 or Isotype control. (A) QQ plot of individual organelle DyLight488 fluorescent intensity distributions. (B) QQ plot of individual organelle electrophoretic mobility distributions. DyLight488 conjugated anti-LC3 antibody (*y*-axis) versus DyLight488 conjugated isotype control (*x*-axis). Markers represent the 5–95th percentiles. Data were acquired using conditions described in Figure 1.

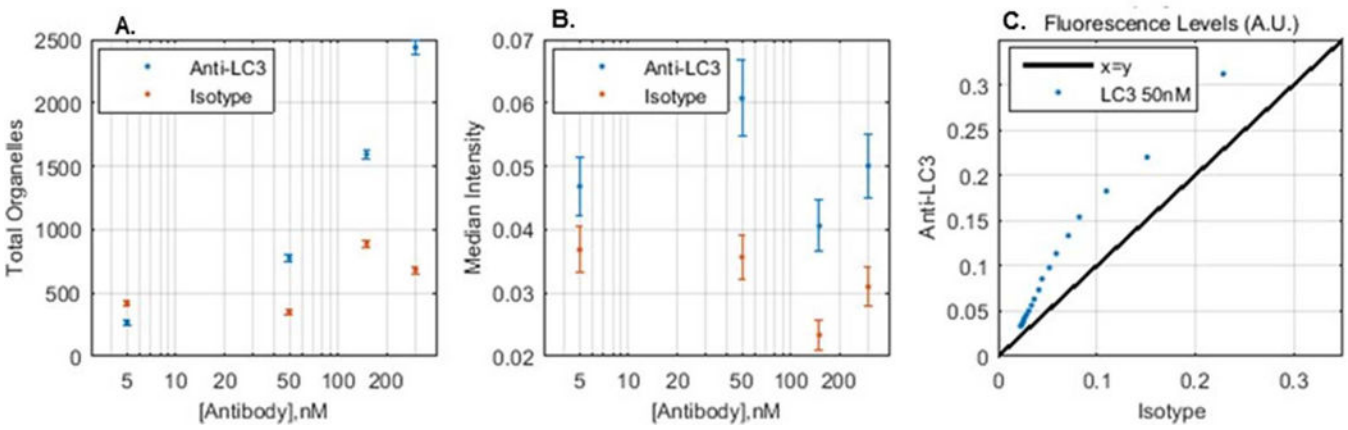

Figure 4.

Selection of DyLight488-conjugated anti LC3 antibody concentration for analysis of autophagy organelles from tissue samples. (A) Total organelle events versus antibody concentration. Error bars represent the Poisson distribution standard error, sqrt(*n*). (B) Median intensity versus antibody concentration. Error bars represent the boundaries of the 40th and 60th percentiles. (C) QQ plot to assess the specificity of 50 nM antibody concentration. DyLight488-conjugated anti-LC3 antibody (*y*-axis) versus DyLight488-conjugated isotype control (*x*-axis). Markers represent the 5th–95th percentiles. Data were acquired using capillary cytometry.

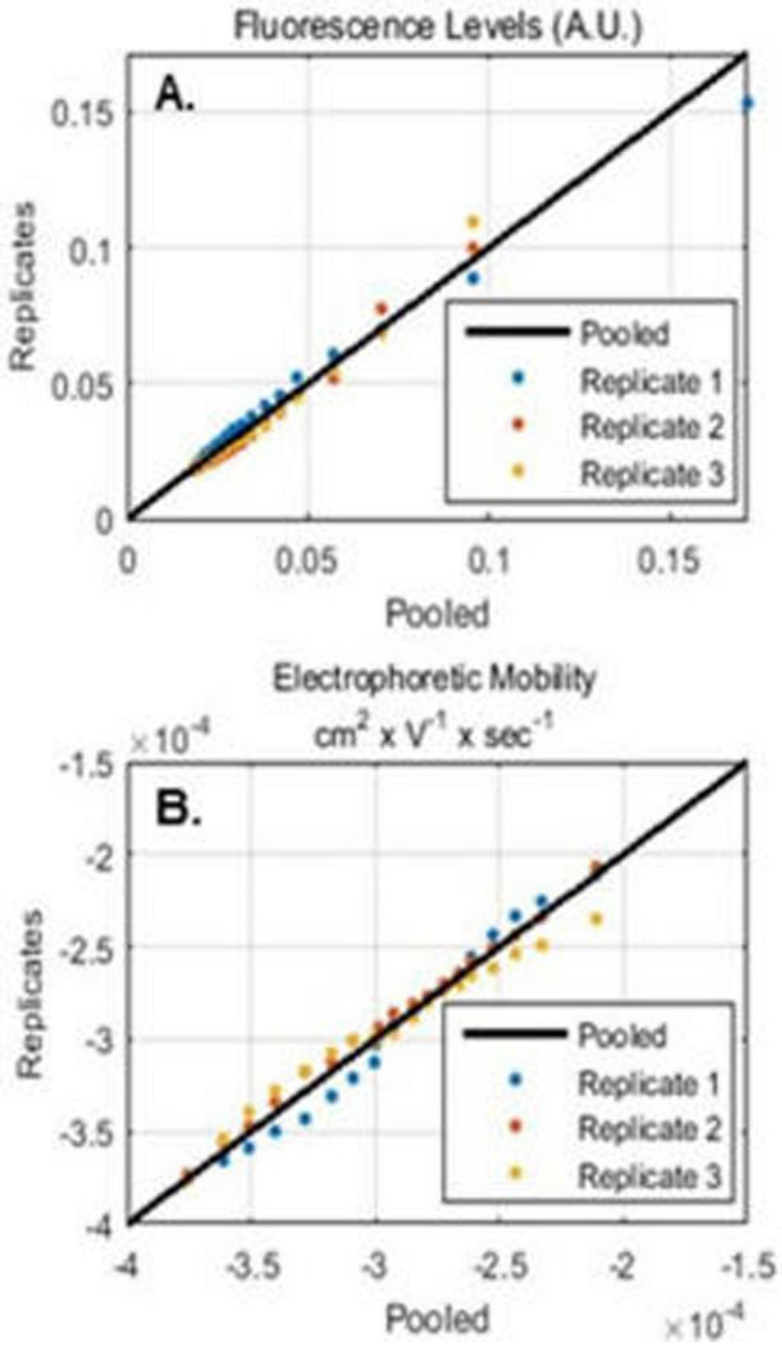

Figure 5.

Reproducibility of technical replicates. (A) DyLight488-conjugated anti-LC3 antibody fluorescence (A.U.) for each technical replicate (*y*-axis) versus the pooled data (*x*-axis). (B) Electrophoretic mobility ($cm^2 \times V^{-1} \times s^{-1}$) for each technical replicate versus the pooled data (*y*-axis). Markers represent the 5–95th percentiles. Data were acquired using conditions described in Figure 1.